Developmental simulation of the adult cranial morphology of *Australopithecus sediba*

AUTHORS:
Keely B. Carlson[1]
Darryl J. de Ruiter[1,2]
Thomas J. DeWitt[3]
Kieran P. McNulty[4]
Kristian J. Carlson[1,5]
Paul Tafforeau[6]
Lee R. Berger[2]

AFFILIATIONS:
[1]Department of Anthropology, Texas A&M University, College Station, Texas, USA
[2]Evolutionary Studies Institute, School of Geosciences, University of the Witwatersrand, Johannesburg, South Africa
[3]Department of Wildlife and Fisheries Sciences, Texas A&M University, College Station, Texas, USA
[4]Department of Anthropology, University of Minnesota, Minneapolis, Minnesota, USA
[5]Department of Anthropology, Indiana University, Bloomington, Indiana, USA
[6]European Synchrotron Radiation Facility, Grenoble, France

CORRESPONDENCE TO:
Keely Carlson

EMAIL:
keelyc@tamu.edu

POSTAL ADDRESS:
Department of Anthropology, Texas A&M University, MS 4352 TAMU College Station, Texas 77845, USA

DATES:
Received: 12 Jan. 2016
Revised: 16 Mar. 2016
Accepted: 17 Mar. 2016

KEYWORDS:
Malapa; geometric morphometrics; craniofacial morphology; hominin evolution; ontogenetic projection

HOW TO CITE:
Carlson KB, De Ruiter DJ, DeWitt TJ, McNulty KP, Carlson KJ, Tafforeau P, et al. Developmental simulation of the adult cranial morphology of *Australopithecus sediba*. S Afr J Sci. 2016;112(7/8), Art. #2016-0012, 9 pages. http://dx.doi.org/10.17159/sajs.2016/20160012

The type specimen of *Australopithecus sediba* (MH1) is a late juvenile, prompting some commentators to suggest that had it lived to adulthood its morphology would have changed sufficiently so as to render hypotheses regarding its phylogenetic relations suspect. Considering the potentially critical position of this species with regard to the origins of the genus *Homo*, a deeper understanding of this change is especially vital. As an empirical response to this critique, a developmental simulation of the MH1 cranium was carried out using geometric morphometric techniques to extrapolate adult morphology using extant male and female chimpanzees, gorillas and humans by modelling remaining development. Multivariate comparisons of the simulated adult *A. sediba* crania with other early hominin taxa indicate that subsequent cranial development primarily reflects development of secondary sexual characteristics and would not likely be substantial enough to alter suggested morphological affinities of *A. sediba*. This study also illustrates the importance of separating developmental vectors by sex when estimating ontogenetic change. Results of the ontogenetic projections concur with those from mandible morphology, and jointly affirm the taxonomic validity of *A. sediba*.

Introduction

To date, only a single, relatively complete cranium of *Australopithecus sediba* has been recovered from the Malapa fossil site, belonging to the type specimen MH1.[1] Dating to 1.977±0.002 Ma,[2] the Malapa hominins exhibit a unique, mosaic morphology, possessing features that align them with both the genus *Homo* as well as other species of australopith[1]. Based on this intermediate morphology, Berger et al.[1] suggested a possible ancestor–descendant relationship between *A. sediba* and the genus *Homo*, with the possibility of *A. sediba* representing the direct ancestor to *H. erectus*, or otherwise a close sister group to that ancestor. The cranium itself shows remarkable preservation, possessing a complete facial skeleton and detailed surface anatomy with clearly visible suture lines. The second molars are in occlusion in this specimen, while the third molars remain in the crypt[1], indicating its sub-adult status. With an estimated cranial capacity of 420 cm^3, it is estimated that MH1 had achieved approximately 95% of its expected brain growth at age of death.[1,3]

In response to the announcement, several outside commentators immediately questioned the distinctiveness of *A. sediba* as a unique species separate from *A. africanus*.[4,5] In a diametrically opposed argument, others suggest that this species should have been assigned to the genus *Homo*.[4] Because of the young age and hence incomplete growth of the type specimen, several commentators have further questioned the reliability of phylogenetic interpretations based on the MH1 fossil.[4-8] Critics of the Berger et al.[1] interpretations argue that the degree of development expected to occur between second and third molar eruption would have been substantial enough to alter our current interpretations of the morphological affinities of *A. sediba*, especially those features thought to resemble later *Homo*. For example, Spoor[6] argued the possibility for increased constriction of the MH1 brain case had it reached full adulthood. More recently, Kimbel[8] criticised the use of the juvenile mandible in multivariate statistical comparisons with other species, based on the potential of continued growth and development for impacting linear measurements.[9]

To address this possibility, we used established geometric morphometric techniques[10-16] to produce 3D renderings of the inferred adult cranial morphology of *A. sediba* based on regression of developmental samples in accordance with dental eruption sequence, or dental stage. The goal of this procedure was to generate a series of developmental trajectories for both male and female extant apes and humans (Table 1), and then apply these trajectories to MH1 to create a series of virtual adult crania. This procedure, in turn, allowed us to empirically establish the estimated adult form of *A. sediba*, and test whether or not current interpretations regarding the cranial morphology of this species should be modified as a result of future developmental changes.

Table 1: Summary of hominoid sample used to create developmental vectors

Species	Juveniles†	Male adults‡	Female adults‡
Pan troglodytes	13	6	7
Gorilla gorilla	15	6	4
Homo sapiens	8	16	11

†M2 indicates second molars are erupted and in occlusion; ‡M3 indicates that the third molars are erupted and in occlusion.

Materials and methods

Reconstruction

A reconstruction of the MH1 cranium was carried out with the goal of correcting for distortion in the cranium and producing a more complete rendered model of the *A. sediba* skull (Figure 1a,b). Rapidform® software (now 3D Systems Geomagic; see http://www.rapidform.com/home) was employed in this reconstruction to refine and process 3D models. The original 3D model of the MH1 cranium employed in this reconstruction was created using synchrotron image data generated on the beamline ID17 at the European Synchrotron Radiation Facility located in Grenoble, France.[17] Synchrotron image data were segmented using Avizo 6.3® software, resulting in a 3D virtual rendering of the MH1 cranium, removed from the encasing breccia.[17] This imaging allowed for the collection of landmark data in areas that were previously obscured by matrix.

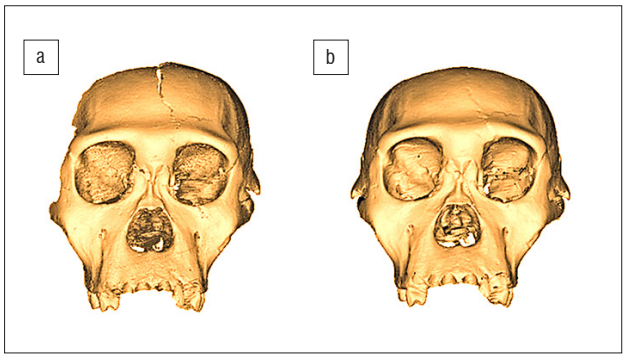

Figure 1: MH1 cranium (a) before and (b) after reconstruction.

When examining the juvenile cranium, several preservation issues impacting the integrity of the fossil were apparent. The most prominent among these is a large crack, originating at the left supraorbital torus, which runs posteromedially across the frontal, widening as it continues to bregma to reach a maximum breadth of approximately 7 mm. An additional crack affecting landmark placement extends from the medial margin of the right orbit, inferomedially across the frontal process of the maxilla, breaking across the nasal bridge. Best viewed from frontal perspective, the crack obscures the right frontomaxillary suture and laterally displaces the inferior portion of both nasals.

Entire cranial bones were also displaced. As discussed above, the large crack extending across the frontal has resulted in the displacement of the left portion of the frontal bone. The displacement extended laterally from above the left orbit to the articulation with the zygomatic bone. The zygomatic bone was displaced posteroinferiorly, disarticulating the bone from the zygomatic arch of the temporal and the zygomatic process of the frontal. This distortion can also be noted from the frontal aspect when examining the inferior margin of the left orbit. Reconstruction correcting for the cracks and displacements as just described was a major focus of the present project. An additional goal was to produce a more complete calvaria by reflecting the preserved portions of the left parietal and temporal bones. Fortunately, any plastic deformation was deemed extremely minor, if present at all.

The 3D model of the MH1 cranium was first imported into Rapidform®, and all adjustments were conducted in 'mesh mode'. It was decided that the most efficient and effective way to account for cracks and displacements was by selecting the affected areas that required adjustment, copying and pasting these regions into a separate window, and then re-aligning the selected area with the original model. The selected areas were reoriented using the 'scan tools' property and 'align between scan data'. Using these tools, one selects a reference scan and a moving scan, which are then aligned in accordance with selected analogous points that serve to stitch the scans together.

To correct for the large crack across the frontal bone, we first selected the preserved portions of the frontal, parietal, sphenoid and temporal bones extending to the left of the crack. These portions were then copied into a separate window and selected as the moving scan to align with the remaining portion of the cranium using the 'align between scan data' tool. Once the crack had been corrected, we were then able to move and realign the zygomatic using the same process, in which the zygomatic bone was removed and then rearticulated with the zygomaticotemporal and zygomaticofrontal sutures. The portion of the nasal bones laterally displaced inferior to the break was additionally removed and realigned using the same process used for correcting the zygomatic and frontal bones.

The mirror tool was used to correct for the distortion along the nasal bridge, by reflecting the left side of the superior portion of the nasal bridge to remove the crack across the frontomaxillary suture. After correcting for displacement and distortion in the cranium, the mirror tool was used to reflect the left half of the calvaria posterior to the coronal suture to produce a more complete calvaria. As a final step in the reconstruction, the scans from the corrected model were then merged into a single scan and the resulting model was run through 'global remesh'. This command regenerates the mesh structure with removed defects in accordance with the model's curvature flow. A final product is shown in Figure 1b.

Sample

A summary of the hominoid comparative samples – comprising male and female chimpanzees (*Pan troglodytes*), gorillas (*Gorilla gorilla gorilla*) and modern humans (*Homo sapiens*) – is listed in Table 1. Ape data were collected from wild-shot specimens housed at the Cleveland Museum of Natural History (Cleveland, OH, USA). Records for chimpanzees indicate that specimens were collected in Ebolwa, Cameroon, as well as Abong Mbong, French Cameroons, and Abong Mbong, Djaposten, Cameroons, West A, with the exception of three specimens for which no geographical data are available. The records for the gorilla crania used in the comparative sample indicate that specimens were collected in French West Africa, French Congo, Ebolwa, Cameroon, Abong Mbong, French Cameroons, and Abong Mbong, Djaposten, Cameroons, West A. Both chimpanzee and gorilla crania were sexed using cranial remains. The human sample primarily included cadaver crania obtained from the Raymond A. Dart Collection of Human Skeletons at the School of Anatomical Sciences at the University of the Witwatersrand (Johannesburg, South Africa), although several well-preserved archaeological crania were included from both the Raymond A. Dart Collection of Human Skeletons and the Cleveland Museum of Natural History. Specimens with obvious pathologies or abnormalities were excluded from the study sample. Archaeological crania were only used if they could be confidently sexed using available records or standard cranial sexing criteria.

Specimens were assigned to developmental categories based on dental eruption sequence. Sub-adults were judged to be of the same developmental age as MH1, and therefore suitable for inclusion within the study, if the second molars were erupted and in occlusion, while the third molars had not yet erupted. Specimens were designated as adults if the third molars were erupted and in occlusion. Both male and female specimens were sampled for parity, although the juvenile sample was pooled for the purpose of developmental simulation. Considerable research has been conducted on both the timing and development of sexual dimorphism among hominoids.[18-21] Results of this research indicate that differences in craniofacial morphology of great apes and humans is established early in ontogeny.[20] Research further identifies the effects of allometric scaling, as well as disparities in growth rates and growth spurts of male and female hominoids as considerable influences in the onset and resulting degree of sexual dimorphism among species.[18,19,21] However, as a result of both the limited number of juveniles, and the fact that sex was often unknown for these specimens, we maintain that pooling of the juvenile sample was appropriate in the present study. We further note that previous studies employing developmental simulation have used pooled juvenile samples for similar reasons.[13]

The hominin fossil sample used in geometric morphometric comparative analyses included a sample of non-'robust' australopith and early

Homo crania from five species: *A. sediba* (MH1), *A. africanus* (Sts 5, Sts 71, Stw 53), *H. habilis* (OH 24, KNM-ER 1813), *H. rudolfensis* (KNM-ER 1470) and *H. erectus* (D2700, KNM-WT 15000, KNM-ER 3733). Laser surface scans of *A. africanus* fossils were collected from original fossil material at the Ditsong Museum of Natural History in Pretoria, South Africa. The original OH 24 fossil, referred to as *H. habilis*, was scanned at the National Museum of Tanzania in Dar es Salaam. Scans from the Dmanisi and Kenyan fossil material were obtained from casts, as the original fossil material was not available.

Methods

The ontogenetic samples for extant chimpanzees, gorillas and humans and fossil hominin crania were collected using a NextEngine 3D laser scanner®. Surface scans were stitched together and fused using Scanstudio HD Pro software®. These scans were later imported into Geomagic® where they were smoothed and polished using the 'mesh doctor' tool. 'Mesh doctor' provides an automatic polygon mesh improvement tool, which both detects errors in the mesh and corrects them. All holes in the mesh were filled-in using Geomagic® to prevent any landmarks or semi-landmarks from 'falling through' the mesh during landmark placement.

After fusing and polishing, each scan was imported into Landmark Editor 3.6®[22] software where 76 traditional landmarks and semi-landmarks were then placed (Table 2). Three semi-landmark curves were placed along the mid-sagittal plane between rhinion and bregma. These landmarks were not slid, but rather served as traditional landmarks. Landmark files for each hominoid species were exported to MorphoJ®[23] software where they were aligned through generalised Procrustes analysis. Generalised Procrustes analysis minimises the sum of squared distances between homologous points on each specimen and the imputed mean configuration through translation, rotation and scaling, thus controlling for the effects of location, orientation and size within the sample.[24-27] Estimated adult MH1 crania produced from each ontogenetic trajectory (male and female chimpanzee, gorilla and human) were visualised in Landmark Editor 3.6® software[22] using thin-plate spline interpolations of the corrected MH1 cranial surface warped into the estimated adult configuration (Figure 2a,b).

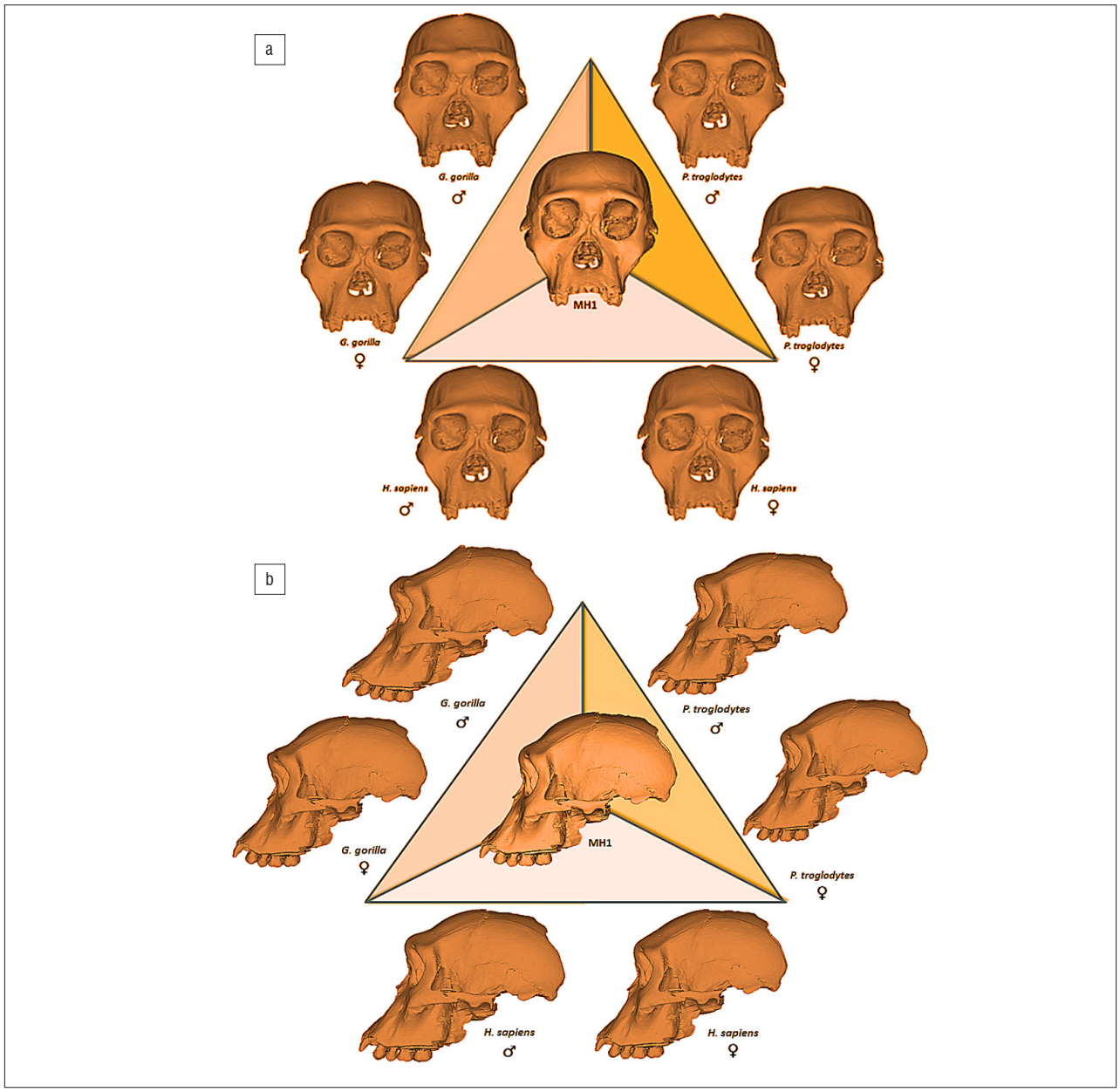

Figure 2: Visualisations of MH1 and its simulated adult forms from hominoid developmental trajectories in (a) frontal and (b) lateral aspects.

Table 2: Landmark definitions for landmarks used in developmental simulation

Landmark	Definition
1,2	Mid-torus inferior (right and left)
3,4	Mid-torus superior (right and left)
5,6	Dacryon (right and left)
7,8	Zygoorbitale (right and left)
9,10	Frontomalare orbitale (left and right)
11,12	Infraorbital foramen (right and left)
13,14	Zygomaxillare (right and left)
15,16	Alare (right and left)
17	Anterior attachment of nasal septum
18	Prosthion
19,20	I1-I2 contact (left and right)
21,22	I2-canine contact (left and right)
23,28	Canine-P3 contact
24,29	P3-P4 contact
25,30	P4-M1 contact
26,31	M1-M2 contact
27,32	M2-M3 contact
33,34	Jugale (left and right)
35	Zygomatico-temporal suture superior
36	Zygomatico-temporal suture inferior
37,38	Pterion
39,40	Inferior-most point of post-glenoid process
41	Incisivion
42	Alveolon
43,44	Inferolateral junction of nasal with maxilla (right and left)
45,46	Frontomalare temporale (left and right)

Note: In addition to the landmarks listed here, three curves of semi-landmarks were added along the mid-sagittal curve between rhinion and bregma, with a density of 10 equidistant spaced semi-landmarks each, making for a total of 76 landmarks. Curve one begins at rhinion and ends at the posterior junction of the glabella and the slope of the frontal bone. Curve two begins at this point and ends at the midpoint along the mid-sagittal curve of the frontal bone. Curve three begins at this midpoint on the frontal bone and ends at bregma.

A subset of 32 landmarks across the calvaria, face and palate of specimens was then used for morphometric comparisons between hominin crania and simulated versions of *A. sediba* individuals (Table 3). Producing this subset was necessary for comparing extant taxa landmarks to landmarks obtainable on the occasionally incomplete fossil specimens selected for analysis. In order to include specimens Sts 71 and KNM-WT 15000, missing landmarks were estimated through reflection of antimeres.

Table 3: Landmark definitions for the subset of landmarks used in morphometric comparison

Landmark	Definition
1	Rhinion
2	Nasion
3	Glabella
4	Bregma
5	Anterior attachment of nasal septum
6	Prosthion
7,8	Mid-torus inferior (right and left)
9,10	Mid-torus superior (right and left)
11,12	Frontomalare orbitale (left and right)
13,14	Frontomalare temporale (left and right)
15,16	Dacryon (left and right)
17,18	Zygoorbitale (right and left)
19,20	Zygomaxillare (right and left)
21,22	Alare (right and left)
23,24	Malar root origin (right and left)
25,26	I1-I2 contact
27,28	C-P3 contact
29	Incisivion
30	Alveolon
31	Left distal palate
32	Right distal palate

Principal component analysis (PCA) of covariances was conducted on the Procrustes shape coordinates using the subset of 32 landmarks collected from the extant hominoid and fossil sample. The adult gorilla sample was excluded from the PCA because of concerns that, if included, these specimens would largely distort the results as a result of their more divergent morphology compared to other species included in the sample.[18,21,28] Analyses were conducted both with and without the extant hominoids to control for the likely dominance of these samples in driving definition of the major principal component axes. In other words, one could ask, to what extent was the position of the fossil specimens affected by the ordination of modern chimpanzees and humans in the same data space? To control for this effect, we also conducted a PCA using only fossil specimens to assess the distribution of crania in the context of fossil hominin variation.

Average Procrustes chord distances both within and between taxa were also calculated using Excel software on the subset of 32 landmarks for the same chimpanzee, human and fossil sample that was used in the PCA. The purpose of this test was to determine if the overall distance within the *A. sediba* sample (i.e. intragroup variation), including all simulated adults and the reconstructed juvenile cranium, exceeds that observed in extant hominoid species. One can further compare the average distance between *A. sediba* and other individual hominin species to assess group similarities.

Results and discussion

Developmental simulations

Qualitative assessment of the simulated adult crania indicated that the majority of morphological changes expected to occur between second and third molar eruption are related to the development of secondary sexual characteristics (Figure 2a,b). The most significant changes were observed along the male gorilla developmental vector, for which we see the glabella becoming more pronounced, the supraorbital torus thickening, and the zygomatic increasing in its superior-inferior dimension. Increased horizontal angulation, or bending across the mid-face, is also apparent, as is increased lower facial prognathism. Similar transformations were also observed, although to a lesser extent, along the male chimpanzee developmental vector, where one again observes development of moderate lower facial prognathism and a general enhancement of facial robusticity, such as a slight thickening of the supraorbital torus and glabella, as well as a more rugged appearance in the zygomatics. The magnitude of morphological change observed for the female developmental vectors of the gorilla and chimpanzee simulations was comparatively much less. Changes associated with both the male and female human developmental vectors were minimal, producing no notable deviations from the original juvenile form. Thus, while the choice of sex and species did result in observable differences in the estimated adult form of MH1 when applying the chimpanzee and gorilla developmental vectors, applying the human developmental vectors to MH1 resulted in relatively more modest variation in adult simulated form. Given that *A. sediba* evinces a pattern of canine size dimorphism and facial robusticity similar to other australopiths and to early *Homo,*[1,9] we consider the gorilla developmental pattern, in particular that of the male gorilla, to be the least suitable model, while chimpanzee or human developmental patterns would likely provide better estimates of the onset of secondary sexual characteristics in MH1.

Morphometric comparisons

Results of the PCA are illustrated in Figure 3 using adult chimpanzee, human and non-robust hominin crania, including MH1 and its simulated adult conformations. Visualisations of principal component shape change for the first three principal component axes are provided in Figure 4. The first axis of variation is dominated by differences in the length and orientation of the frontal bone, in accordance with the high loading for the bregma landmark, whereas the second axis also summarises changes in cheek morphology, with specimens separated based on the overall gracility or robusticity of the zygomatic. This latter interpretation is based on the high loadings for zygomaxillary landmarks as well as the relative distribution of specimens. The third axis is dominated by differences in morphology of the anterior and posterior palate, with the highest loadings being observed for landmarks in this region. These interpretations correspond to the visualisations of shape change for each axis provided in Figure 4.

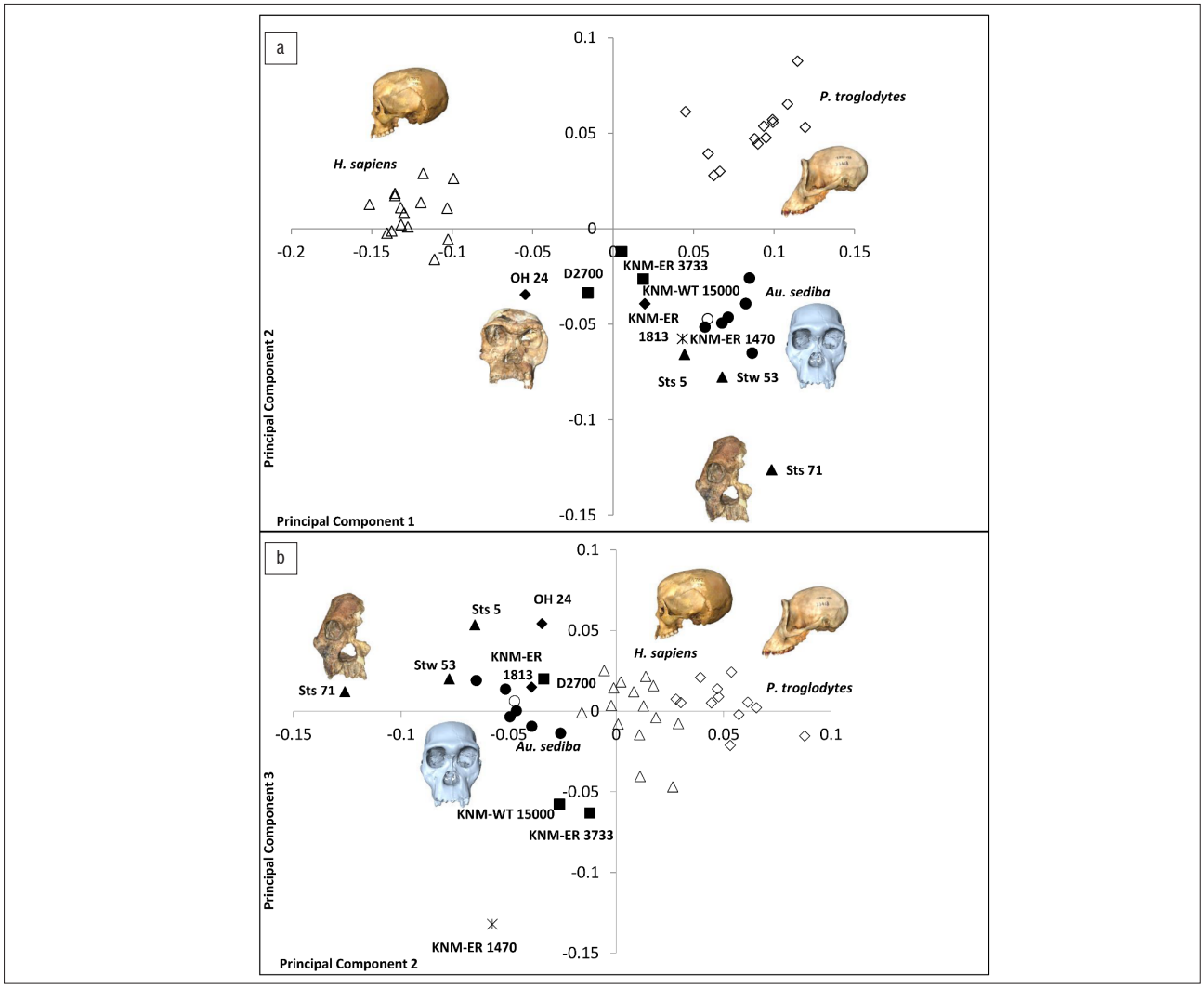

A. africanus *(filled triangles);* A. sediba *simulated adults (filled circles); MH1 juvenile (open circle);* Homo habilis *(filled diamonds);* H. rudolfensis *(star);* H. erectus *(filled squares);* H. sapiens *(open triangles);* Pan troglodytes *(open diamonds).*

Figure 3: Major (principal component) axes of cranial shape for hominoids, including simulated adult crania of *Australopithecus sediba*. (a) Principal components 1 and 2 (58.7% and 11.0% of variance, respectively). (b) Principal components 2 and 3 (11.0% and 6.5% of total variance, respectively).

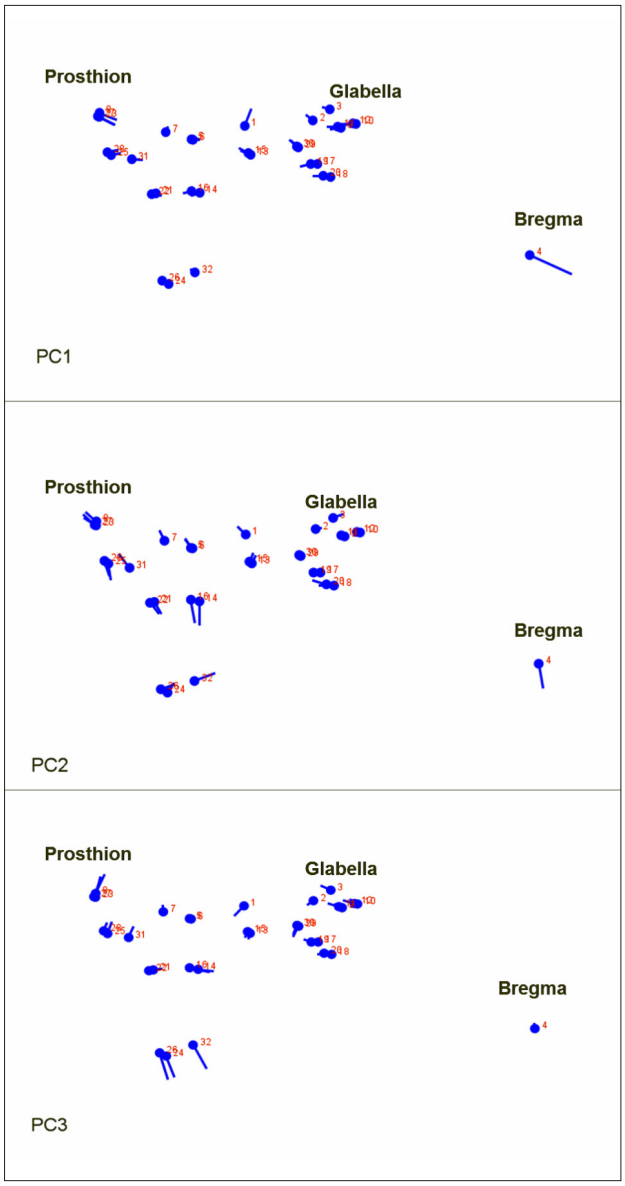

Figure 4: Visualisations of shape change for principal component axes 1–3. Axes correspond to Figure 3.

All six simulated adult *A. sediba* crania – regardless of the species or sex used to estimate them – fall out along both axes with the original, juvenile MH1 cranium in a discrete group relative to other apes or fossil taxa in the analysis (Figure 3a). Early *Homo* crania tend to cluster together with the exception of KNM-ER 1470, which appears to cluster with Sts 5 on the first two major axes (Figure 3a). However, this proximity vanishes when we examine the third principal component, wherein KNM-ER 1470 plots as an outlier (Figure 3b). In addition, considering component 2 versus component 3 (Figure 3b), KNM-ER 1813, OH 24, and the Dmanisi specimen D2700 are separated from *H. erectus sensu lato* crania KNM-WT 15000 and KNM-ER 3733, instead plotting near the cluster of simulated *A. sediba* crania. One outlier to this latter group is the *A. sediba* cranium simulated using a male gorilla developmental vector, which plots in this space nearest the *A. africanus* cranium Stw 53. The exceptional location for the MH1 adult version simulated from male gorillas is not entirely surprising, given that one observes the greatest degree of morphological change when applying this vector, although again we consider a male gorilla-like pattern of development to be the least likely for *A. sediba*. Of perhaps more interest is the fact that a male chimpanzee developmental trajectory makes MH1 appear more similar to early *Homo* and modern humans.

A second PCA on the fossil sample, excluding chimpanzees and humans, is illustrated in Figure 5, with visualisations of shape change for the first three principal component axes provided in Figure 6. Similar to the PCA including chimpanzees and humans, the first axis of variation is dominated by changes in morphology of the frontal bone, but is also influenced by morphological variation of the posterior palate, likely related to the relative degree of facial prognathism among specimens. The second axis is also largely dominated by the morphology of the posterior palate, with high loadings for landmarks in this region. While the *A. sediba* crania generated using chimpanzee and modern human developmental vectors continue to cluster closely to one another, the simulated adult produced from the male gorilla developmental vector shows dissimilarity relative to other *A. sediba* specimens, plotting nearest *A. africanus* specimen Sts 71 (Figure 5a).

As the third principal component also accounts for a substantial amount of the total variation (15.2%) in the PCA using only fossils, we examined the distribution of fossil taxa along this axis. This third axis of variation was also influenced primarily by changes in the frontal bone and palate. When comparing principal component 2 versus component 3, all *A. sediba* estimated adults, along with the original juvenile cranium, clustered together, separated from *A. africanus* and other hominin taxa along the third axis of variation (Figure 5b).

The results of the above PCA are supported across the full shape space by an analysis of shape differences within and among taxa using average Procrustes distances (Table 4). Examination of the Procrustes chord distances indicates that the within-species variation for *A. sediba* simulated adults and the juvenile cranium is actually less than that of the modern human and chimpanzee samples used in the study.

Conclusions

The results of this study support the hypothesis that the expected degree and nature of development that would have occurred between second and third molar eruption in MH1 would not have been substantial enough relative to other hominin taxa to alter our current craniofacial understanding of the phylogenetic relationships of *A. sediba*. In other words, had MH1 lived to adulthood, its craniofacial morphology would look similar enough to its present, juvenile cranial morphology that we can reliably differentiate the taxon using the cranium of this particular specimen. Any future changes would likely be related to the onset of puberty, and the concomitant development of secondary sexual characteristics. As a result, this study further reinforces the importance of separating developmental vectors by sex to avoid obscuring this type of variation in ontogenetic projections.

The fact that the juvenile MH1 cranium continues to cluster with simulated *A. sediba* adults in PCAs conducted in this study reinforces the above position. While we cannot ultimately rule out the scenario that qualitative apomorphies shared with other fossil taxa (e.g. *A. africanus*) might have developed and become expressed only during this later stage of ontogeny, the expression of such features in developmentally much younger fossil hominin specimens[29,30] argues against the likelihood of this possibility. For example, anterior pillars are already present and easily observable in the Taung child, for which only the first molars are in occlusion.[30] Therefore, the late juvenile status of the type specimen, MH1, would not likely influence our diagnosis of this species. These traits on the reconstructed cranium of MH1 and its ontogenetic simulated extrapolations concur with those for the mandibles of MH1 and MH2.[9] Both studies indicate the verity of *A. sediba* as a unique taxon. Based upon our current understanding of the postcranial anatomy of the Malapa hominins, which indicates an *Australopithecus*-level adaptive grade, the *Homo*-like features observed in the simulated adults generated when applying the *H. sapiens* and *P. troglodytes* trajectories reinforce the transitional nature of this species.

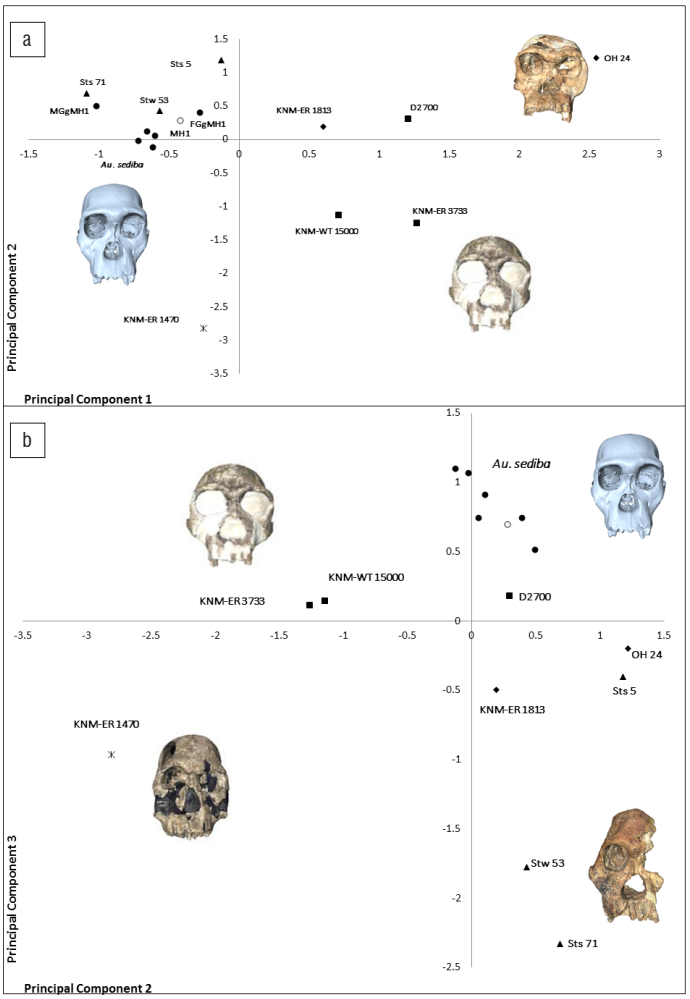

Australopithecus africanus *(filled triangles);* A. sediba *simulated adults (filled circles); MH1 juvenile (open circle);* Homo habilis *(filled diamonds);* H. rudolfensis *(star);* H. erectus *(filled squares).*

MGgMH1 indicates the adult A. sediba *specimen generated from the male gorilla developmental vector; FGgMH1 indicates the adult* A. sediba *specimen generated from the female gorilla developmental vector.*

Figure 5: Major (principal component) axes of cranial shape for non-robust fossil crania. (a) Principal components 1 (28.3% of variance) and 2 (21.7% of variance). (b) Principal components 2 and 3 (15.2% of variance).

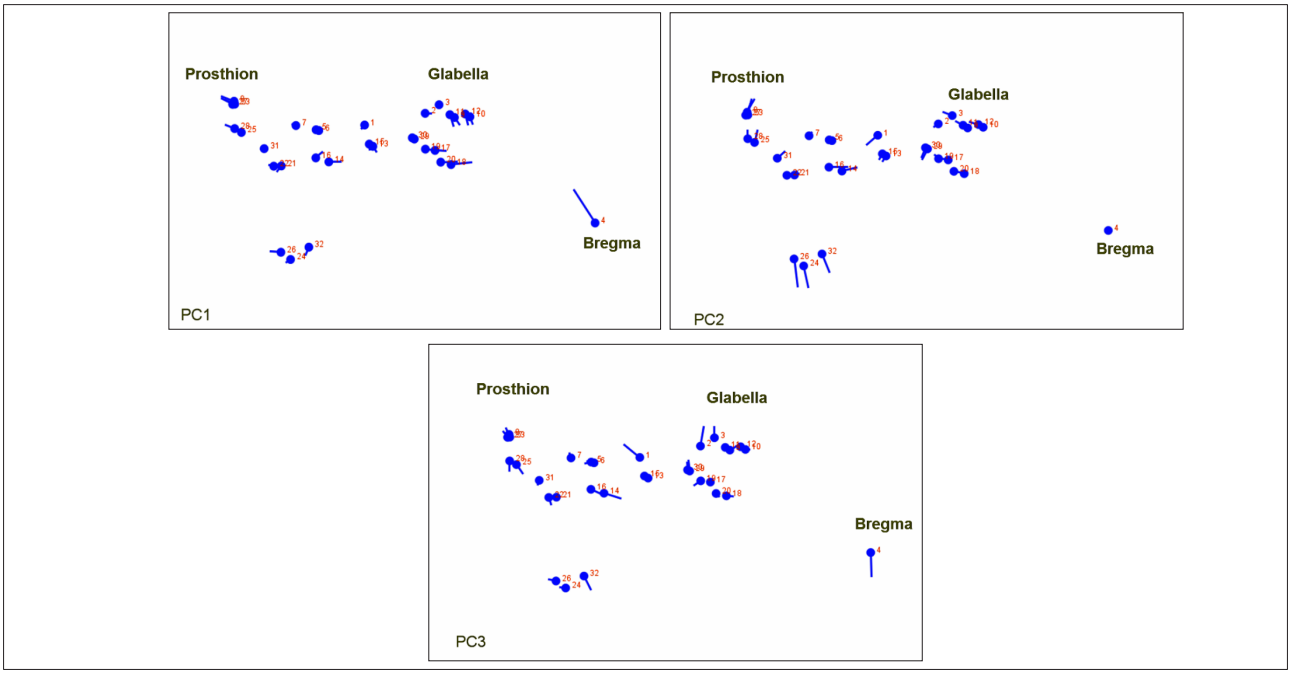

Figure 6: Visualisations of shape change for principal component axes 1–3. Axes correspond to Figure 5.

Table 4: Average Procrustes chord distances within taxa (on diagonal) and among taxa (off diagonal)

	Australopithecus africanus	*Australopithecus sediba*	*Homo erectus*	*Homo habilis*	*Homo sapiens*	*Pan troglodytes*	*Homo rudolfensis*
A. africanus	**0.145**						
A. sediba	0.101	**0.059**					
H. erectus	0.138	0.112	**0.144**				
H. habilis	0.137	0.138	0.098	**0.163**			
H. sapiens	0.226	0.21	0.149	0.146	**0.089**		
P. troglodytes	0.152	0.11	0.133	0.159	0.218	**0.092**	
H. rudolfensis	0.188	0.173	0.158	0.208	0.236	0.2	–

Bolded numbers indicate average within species variation. The range of variation within P. troglodytes *is 0.0597–0.14093. The range of variation within* H. sapiens *is 0.06654–0.12589. Distances were calculated using Excel software for the subset of 32 landmarks collected from the adult* P. troglodytes, H. sapiens *and fossil sample.*

Acknowledgements

We thank the South African Heritage Resource agency for permits to work on the Malapa site, and the Nash family for granting access to the Malapa site and the continued support of research on their reserve. The South African Department of Science and Technology, and the African Origins Platform, the South African National Research Foundation, the Evolutionary Studies Institute, the Palaeontological Scientific Trust, the Andrew W. Mellon Foundation, the United States Diplomatic Mission to South Africa, the National Geographic Society, the A. H. Schultz Foundation, the Oppenheimer and Ackerman families, Sir Richard Branson, Sigma Xi, Texas Academy of Science, Vision 2020 Dissertation Enhancement Award of Texas A&M University, and the Program to Enhance Scholarly and Creative Activities and the International Research Travel Award Grant of Texas A&M University all provided funding for this research. D.J.d.R. holds a Liberal Arts Cornerstone Faculty Fellowship at Texas A&M University, which provided additional funding. The University of the Witwatersrand's Schools of Geosciences and Anatomical Sciences and the Evolutionary Studies Institute provided support and facilities. We thank the European Synchrotron Radiation Facility for granting beam time on ID17 for experiment #EC521. We thank E. Mbua, P. Kiura, V. Iminjili, and the National Museums of Kenya, Dr. P. Msemwa and the National Museum and House of Culture of Tanzania, S. Potze of the Ditsong Museum, B. Billings of the School of Anatomical Sciences of the University of the Witwatersrand, W. Seconna of the Iziko South African Museum, and L.M. Jellema of the Cleveland Museum of Natural History for access to comparative fossil and extant primate and human materials in their care. Numerous individuals have been involved in the ongoing preparation and excavation of these fossils including C. Dube, B. Eloff, C. Kemp, M. Kgasi, M. Languza, J. Malaza, G. Mokoma, P. Mukanela, T. Nemvhundi, M. Ngcamphalala, S. Jirah, S. Tshabalala and C. Yates. Other individuals who have given significant support to this project include B. de Klerk, C. Steininger, B. Kuhn, L. Pollarolo, B. Zipfel, J. Kretzen, D. Conforti, J. McCaffery, C. Dlamini, H. Visser, R. McCrae-Samuel, B. Nkosi, B. Louw, L. Backwell, F. Thackeray, M. Peltier, J. Soderberg and D. Roach. The *A. sediba* specimens are archived at the Evolutionary Studies Institute at the University of the Witwatersrand. All data used in this study are available upon request, including access to the original specimens, by bona fide scientists.

Authors' contributions

All authors contributed to the work presented in this paper and the writing of the document. K.B.C., D.J.d.R., T.J.D. and K.P.M. conceived the project. K.B.C., T.J.D. and K.P.M. carried out all statistical analyses and comparisons of the MH1 fossil and simulated adults. P.T. and L.R.B. carried out the synchrotron scan of the MH1 fossil cranium. K.J.C. analysed and segmented the synchrotron scan data providing the 3D model that was used for reconstruction and comparison. K.B.C. and K.P.M. reconstructed the synchrotron scan of the MH1 cranium, correcting for cracks and displacements in the fossil.

References

1. Berger LR, De Ruiter DJ, Churchill SE, Schmid P, Carlson KJ, Dirks PHGM, et al. *Australopithecus sediba*: A new species of *Homo*-like australopith from South Africa. Science. 2010;328:195–204. http://dx.doi.org/10.1126/science.1184944
2. Pickering R, Dirks PHGM, Jinnah Z, De Ruiter DJ, Churchill SE, Herries AIR, et al. *Australopithecus sediba* at 1.977 M and implications for the origins of the genus *Homo*. Science. 2011;333:1421–1423. http://dx.doi.org/10.1126/science.1203697
3. Tobias PV. The brain in hominid evolution. New York: Columbia University Press; 1971.
4. Balter M. Candidate human ancestor from South Africa sparks praise and debate. Science. 2010;328:154–155. http://dx.doi.org/10.1126/science.328.5975.154
5. Cherry M. Claim over 'human ancestor' sparks furore. Nature. 2010 April 08; News. http://dx.doi.org/10.1038/news.2010.171
6. Spoor F. Malapa and the genus *Homo.* Nature. 2011;478:44–45. http://dx.doi.org/10.1038/478044a
7. Wood B, Harrison T. The evolutionary context of the first hominins. Nature. 2011;470:347–352. http://dx.doi.org/10.1038/nature09709
8. Kimbel WH. Hesitation on hominin history. Nature. 2013;497:573–574. http://dx.doi.org/10.1038/497573a
9. De Ruiter DJ, DeWitt TJ, Carlson KB, Brophy JK, Schroeder L, Ackermann RR, et al. Mandibular remains support taxonomic validity of *Australopithecus sediba*. Science. 2013;340(6129). http://dx.doi.org/10.1126/science.1232997
10. McNulty KP, Frost SR, Strait DS. Examining affinities of the Taung child by developmental simulation. J Hum Evol. 2006;51:274–296. http://dx.doi.org/10.1016/j.jhevol.2006.04.005
11. Neubauer S, Gunz P, Hublin J. Endocranial shape changes during growth in chimpanzees: A morphometric analysis of unique and shared aspects. J Hum Evol. 2010;59:555–566. http://dx.doi.org/10.1016/j.jhevol.2010.06.011
12. Gunz P, Neubauer S, Maureille B, Hublin JJ. Brain development after birth differs between Neanderthals and modern humans. Curr Biol. 2010;20:921–922. http://dx.doi.org/10.1016/j.cub.2010.10.018
13. Singleton M, McNulty KP, Frost SR, Soderberg J, Guthrie EM. Bringing up baby: Developmental simulation of the adult cranial morphology of *Rungwecebus kipunji*. Anat Rec. 2010;293:388–401. http://dx.doi.org/10.1002/ar.21076
14. Gunz P, Bulygina E. The Mousterian child from TeshikTash is a Neanderthal: A geometric morphometric study of the frontal bone. Am J Phys Anthropol. 2012;149:365–379. http://dx.doi.org/10.1002/ajpa.22133
15. Gunz P, Neubauer S, Golovanova L, Doronichev V, Maureille B, Hublin JJ. A uniquely modern human pattern of endocranial development. Insights from a new cranial reconstruction of the Neandertal newborn from Mezmaiskaya. J Hum Evol. 2012;62:300–313. http://dx.doi.org/10.1016/j.jhevol.2011.11.013

16. Scott N, Neubauer S, Hublin JJ, Gunz P. A shared pattern of postnatal endocranial development in extant hominoids. Evol Biol. 2014;41:572–594. http://dx.doi.org/10.1007/s11692-014-9290-7

17. Carlson KJ, Stout D, Jashashvili T, De Ruiter DJ, Tafforeau P, Carlson K, et al. The endocast of MH1, *Australopithecus sediba*. Science. 2011;333:1402–1407. http://dx.doi.org/10.1126/science.1203922

18. Shea BT. The ontogeny of sexual dimorphism in the African apes. Am J Primatol. 1985;8:183–188. http://dx.doi.org/10.1002/ajp.1350080208

19. Shea BT. Ontogenetic approaches to sexual dimorphism in anthropoids. Hum Evol. 1986;1(2):97–110. http://dx.doi.org/10.1007/BF02437489

20. Mitteroecker P, Gunz P, Bernhard M, Schaefer K, Bookstein FL. Comparison of cranial ontogenetic trajectories among great apes and humans. J Hum Evol. 2004;46:679–698. http://dx.doi.org/10.1016/j.jhevol.2004.03.006

21. Schaefer K, Mitteroecker P, Gunz P, Bernhard M, Bookstein FL. Craniofacial sexual dimorphism patterns and allometry among extant hominids. Ann Anat. 2004;186:471–478. http://dx.doi.org/10.1016/S0940-9602(04)80086-4

22. Wiley DF, Amenta N, Alcantara DA, Ghosh D, Kil YJ, Delson E, et al. Evolutionary morphing. Proceedings of IEEE Visualization 2005; 2005 October 23–28; Minneapolis, MN, USA. New York: IEEE; 2005. p. 431–438. http://dx.doi.org/10.1109/VISUAL.2005.1532826

23. Klingenberg CP. MorphoJ: An integrated software package for geometric morphometrics. Mol Ecol Resour. 2011;11(2):353–357. http://dx.doi.org/10.1111/j.1755-0998.2010.02924.x

24. Gower JC. Generalized Procrustes analysis. Psychometrika. 1975;40:33–51. http://dx.doi.org/10.1007/BF02291478

25. Bookstein FL. Size and shape spaces for landmark data in two dimensions. Stat Sci. 1986;1:181–222. http://dx.doi.org/10.1214/ss/1177013696

26. Rohlf FJ. Fitting curves to outlines. In: Rohlf FJ, Bookstein FL, editors. Proceedings of the Michigan Morphometrics Workshop. Special Publication no. 2. Ann Arbor, MI: University of Michigan Museum of Zoology; 1990. p. 167–177.

27. Adams DC, Rohlf FJ, Slice DE. Geometric morphometrics: Ten years of progress following the 'revolution'. Ital J Zool. 2004;71:5–16. http://dx.doi.org/10.1080/11250000409356545

28. O'Higgins P, Dryden IL. Sexual dimorphism in hominoids: Further studies of craniofacial shape differences in *Pan, Gorilla* and Pongo. J Hum Evol. 1993;24:183–205. http://dx.doi.org/10.1006/jhev.1993.1014

29. Clarke RJ. Latest information on Sterkfontein's *Australopithecus* skeleton and a new look at *Australopithecus.* S Afr J Sci. 2008;104:443–449.

30. Rak Y. The australopithecine face. New York: Academic Press; 1984.